ingegneria sismica
International Journal of Earthquake Engineering
Anno XLIII - Num. 2 - 2026

Intelligent Computing for Athlete Training Optimization: Model Design and Analysis

Yangyang Li[1,2] *and You Yang*[3,*]

[1] Wuhan Technical College of Communications, WuHan, 430065, China
[2] Graduate University of Mongolia, Ulaanbaatar, 16052
[3] Wuhan Qingchuan University, WuHan, 430204, China

SUMMARY: *To address issues in athletic training such as load scheduling relying on experience, difficulty in timely quantifying performance fluctuations, and a disconnect between training recommendations and risk identification, this paper proposes PTO-Net, an intelligent computing-based model for optimizing athlete training.Based on publicly available SoccerMon monitoring data, the study unifies external load, internal load, recovery status, and contextual factors at the athlete-day granularity to construct continuous training samples. On this foundation, it achieves joint modeling of risk warning, readiness prediction, and load adjustment. This model utilizes time-series weighting method for depicting the recent changes of training, brings in individual baseline correction to consider the differences in athletes' tolerance ranges, hence generates continuous training suggestions through a multi-task output layer. Experiment outcomes prove that PTO-Net attains the best effect on all main tasks: Risk warning AUC reaches 0.871, Risk F1 reaches 0.793, readiness prediction MAE and RMSE are 4.38 and 5.63 separately, load adjustment MAE is 0.087, and directional consistency ratio is 83.2%, hence all of these are exceed the performance of RF, XGBoost, LSTM, Transformer baseline methods. Three-dimensional response surfaces further point out that the overlapping area of low recovery and high variation corresponds to more obvious suggestions for cutting down training quantity. The outcomes of ablation experiments show that the restoration branch, the single baseline revision, and the time weight together are the foundation of the merits this model has. The method which is put forward in this paper gives continuous support for pre-meeting check, training day arrangement, and recovery monitoring, and thus provides a usable calculation framework for the detailed carrying out of wise choice making in sport training.*

KEYWORDS: *Intelligent computing; Athlete training optimization; Training load monitoring; Recovery status assessment; Individualized training recommendations*

1 Introduction

The competition type sports training, more and more, it is organized around the continuous monitoring, the condition identification, and the individual adjustment, this is instead of the cycle planning which relies on experience. The core question is whether a sports person can take on a certain training burden at a specific phase without breaking the balance between performance improvement, tiredness building-up, and harm possibility. In group motion items and period-based arrangement plans, this kind of balance has very big changeability: sportsmen often have different responses to similar outside work, and the same sportsman hence can also

*Lee20181002@163.com
https://doi.org/10.65102/is2026762
Published: 30 April, 2026

have obvious changes in competition weeks, rest weeks, and strong training stages. Hence, the optimization of training needs to reflect the changed individual baseline conditions, not to depend on fixed formulated rules.

This change has turned into possible because both data obtaining and training choices now take place at far higher frequency. Wearable GPS equipment, inertia sensors, heart-beat measuring instruments, and mobile self-report instruments can catch running distance, acceleration movements, sprint numbers, body effort, sleeping condition, body ache, and preparation condition on an almost every day basis. Under such circumstances, artificial intelligence has entered into the assistance for athletes and the formulation of training plans [1]. Already existing summarizing researches further demonstrate that its usages have already expanded to achievement analysis, athletic medicine, body condition observation, training instruction help, and capable people selection [2]. Even so, the models which exist now are still restricted by data quality, interpretability, and the limited ability of generalization in different training situations[3].

The surveillance of training load still is the foundation for the optimization of training. External load is the term that explains the work which gets done, whereas internal load shows the athlete's physiological and perceptual reaction to that work [4, 5]. The relation between them, however, in actual practice is frequently not stable. Decisions that only depend on outside signs can pass over insufficient recovery, hence decisions that are pushed only by subjective tiredness can make necessary training stimulation become weaker. A useful optimization model hence needs to combine multi-source indexes, hence find changes in personal status, hence adjust training to present recovering ability.

The investigation about intelligent training has more and more put together wearable sensation equipment with machine study. Sensor systems that have AI ability can take out rules from body signs, space location, and movement signals, therefore giving support to the adjustment of training and the prediction of injury [6]. Some researches further combine heart rate, inertia data, and subjective tiredness scores to assess training effect and load balance and to produce management suggestions. Even so, three limitations on model level still exist. Numerous research papers take athlete achievement data as mutually independent sampling points and therefore fail to capture the time-related dependence that exists among training days, competition weeks and recovery cycles. Recommendation results also still stay weakly measured, because most models end at risk forecast or state categorization and depend on rule-based conversions for capacity adjustment. Moreover, model outputs give limited coach-oriented explanation capability, thus making it hard to trace early warnings to load increases, decreased recovery, bad sleep, or difference from an athlete’s past basic level.

These restrictions bring reduction to the actual use value of intelligent models when they are in training situations. Decisions inside sports training are numerous, each person different, and very sensitive to mistakes. Hence, a model is expected by people to accomplish more things than only give out static labels like “high risk” or “low risk.” It ought to point out which variation items are pushing the warning, exhibit how training burden can be modified, and make clear whether the modification can disturb the pre-planned training result.

In the meanwhile, athlete-related data frequently contain health condition, position, physiology signals, and behavior records, which hence makes model putting into use cannot be separated from problems of private information, clearness, prejudice, and responsibility. Currently published review articles have pointed out that artificial intelligence uses in sports already continuously meet ethical worries which are connected with fairness, transparency, personal privacy, and responsibility [7]. Because of this reason, the training optimization models ought not to be evaluated only by the predictive accuracy; The actual putting into use also needs enough explanation ability and operation control.

Based on the above issues, this paper focuses on multi-source state identification and load recommendation generation during athletes' training processes to construct an intelligent computing-based training optimization model.The research objectives of this paper are: to extract features related to external load, internal load, and recovery status from continuous training records to establish individualized temporal state representations for athletes; based on this, to perform injury risk identification, training readiness prediction, and load adjustment recommendations; and to validate the model's effectiveness and deployment value in training optimization tasks through comparative experiments, module ablation, time-window sensitivity analysis, and case explanations.

The contributions of this present paper are mainly embodied in three aspects. First, this research puts together session-level training load, daily recovery condition, and risk marks into athlete condition samples, hence avoiding the one-sided depiction of training condition by a single index. Second, this research has made a design for an intellectual training optimization model which contains time encoding, single baseline correction, danger forecast and load suggestion layers, therefore it extends the model's output from status recognition to actionable training adjustments. Third, in the analysis of results, this paper at the same time inspects prediction accuracy, module contribution degrees, inference efficiency, and interpretability, therefore making the evaluation of model more aligned with the demands of daily training management.

2 Methods

2.1 Data Source and Athlete State Representation

This study uses the public SoccerMon dataset, which contains continuous monitoring records from two teams in the Norwegian Women's Elite Football League during the 2020–2021 season, including recovery self-reports, session data, GPS metrics, heart-rate load, attendance, and injury events. Unlike datasets built around a single exercise signal, it links training stimulus, recovery response, and player availability, which supports modeling of current state, short-term risk, and subsequent training adjustment.

To align the data structure with the actual rhythm of training decisions, this study standardizes the raw records to an "athlete-day" granularity.For multiple training sessions recorded for the same athlete on the same day, the data is first weighted and aggregated based on effective duration; for morning subjective questionnaires, post-session RPE, and self-assessed recovery, the data is aligned by timestamp to the pre- and post-training states of that day; for injury, restricted training, missed training, and competition week information, the daily labels are retained, and changes over the past 3 days and 7 days are supplemented.After this processing, each sample corresponds to a "state snapshot of a specific athlete on a specific training day prior to decision-making," rather than a mixture of discrete observations from different sampling frequencies. To ensure that different monitoring sources converge to the same training decision-making granularity, this paper uniformly constructs the raw records into athlete-day samples, as shown in Figure 1.

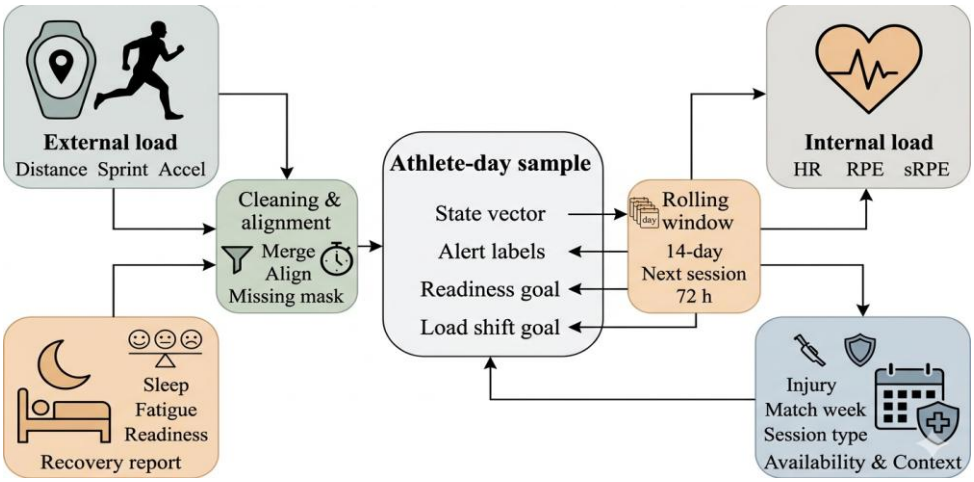

Figure 1: Athlete-day sample construction from multimodal training monitoring

The state of athlete i on training day t consists of four components: external load, internal load, recovery status, and situational control, as shown in Equation (1).

$$x_{i,t} = \left[e_{i,t} \,\|\, u_{i,t} \,\|\, r_{i,t} \,\|\, c_{i,t}\right] \tag{1}$$

where $e_{i,t}$ represents external load, including total running distance, high-speed running distance, number of sprints, number of accelerations, number of decelerations, and player load; $u_{i,t}$ represents internal load, including average heart rate, peak heart rate, post-session RPE, session-RPE, and training intensity; $r_{i,t}$ represents recovery status, including sleep quality, fatigue, soreness, stress, and readiness; $c_{i,t}$ represents contextual control, including session type, location group, days until competition, most recent training interval, and recent training absences [8-13]. Continuous variables are robustly standardized at the athlete-season level; fields with excessively high missing rates are directly excluded, while the remaining variables employ a combined strategy of "nearest-neighbor forward imputation + season median imputation," with missing masks retained.

For making model output results consistent with training management work, this research has defined three objective items: a 72-hour warning sign, preparation degree of next training session, and adjustment range of training load. The final one is measured by the deviation which the external load of the next session has from the average load within the foregoing 7 days, just as what is shown in Equation (2).

$$g_{i,t} = \frac{L_{i,t+1} - \bar{L}_{i,t}^{(7)}}{\bar{L}_{i,t}^{(7)} + \varepsilon} \tag{2}$$

In the equation, $L_{i,t+1}$ represents the comprehensive external load for the next session, $\bar{L}_{i,t}^{(7)}$ represents the average external load over the most recent 7 days prior to the current time point, and ε is a small constant [14-17]. This definition holds both the direction and the magnitude of the adjustment, hence enabling the model to study continuous changes in training suggestions, not crudely cutting adjustment behavior down to simple classification.

For the construction of input, this research utilizes a sliding-window plan with candidate length values of 7, 14, 21, and 28 days, and hence selects the main window via the comparison of validation set. The ultimate time window length is 14 days, which captures load change and recovery alteration near competition times without over-smoothing the recent body condition.

The tensor that we get has kept time sequence, difference between individuals and competition environment. The composition of dataset and the groups of features are all enumerated in Table 1.

Table 1: Dataset Composition and Feature Groups

Feature group	Variables	Main fields
External load	6	total distance, high-speed distance, sprint count, acceleration count, deceleration count, player load
Internal load	5	mean HR, peak HR, RPE, session-RPE, load intensity
Recovery state	5	sleep quality, fatigue, soreness, stress, readiness
Availability and risk	4	injury flag, illness flag, limited participation, missed-session days
Context controls	6	session type, match proximity, position group, weekday, training interval, recent interruption
Derived temporal features	8	3-day mean, 7-day mean, 14-day mean, short-term change, volatility, acute–baseline ratio, last-session gap, missing mask summary

In Table 1, external load, internal load, and recovery status collectively form the primary monitoring layer; availability and contextual variables are used to account for differences in competition schedules, positions, and training organization; derived temporal features are used to supplement the characterization of recent fluctuations in single-day samples.

2.2 Intelligent Training Optimization Model

After sample construction was completed, this paper developed the PTO-Net. The model consists of four components: multi-source input mapping, temporal representation extraction, individual baseline correction, and multi-task output. The design focus is not on increasing network depth, but on enabling the model to stably identify the combined effects of short-term load disturbances, insufficient recovery, and individual baseline shifts on training recommendations.The application of the PTO-Net information coupling mechanism in athlete training optimization is illustrated in Figure 2.

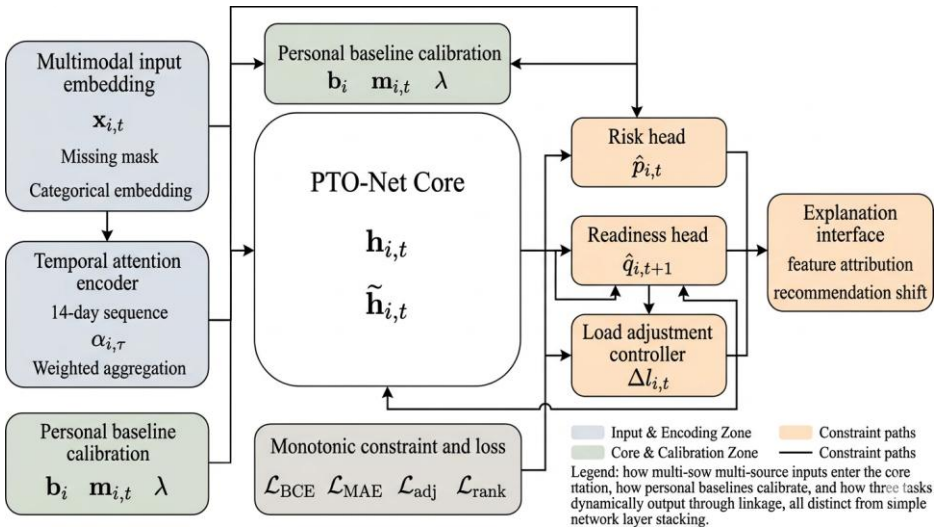

Figure 2: Information coupling mechanism of PTO-Net for athlete training optimization

The multi-source input mapping layer projects continuous features, categorical encodings, and missing-value masks into a unified representation space, after which temporal features are extracted over the 14-day window. Because competition weeks, recovery sessions, and high-intensity sessions contribute differently to later decisions, the model assigns learnable weights to each time step. The final integrated temporal representation is given in Equation (3).

$$h_{i,t} = \sum_{\tau=t-w+1}^{t} \alpha_{i,\tau} \, W x_{i,\tau} \tag{3}$$

In the equation, w represents the input window length, $\alpha_{i,\tau}$ represents the weight at the τth time step, W represents the input mapping matrix, and $h_{i,t}$ represents the composite state representation at the end of the window [18-22]. With this approach, the model can distinguish "short-term spikes," "continuous accumulation," and "insufficient recovery" as distinct temporal patterns, rather than treating the entire historical record as equally important.

Only the temporal expression is not enough to give the personalized training suggestion. Because athletes have differences in basic body condition, competition position and load bearing ability, therefore same running amount and tiredness value can mean different danger degrees. In order to cope with this situation, the model carries out individual baseline correction after temporal encoding through the combination of the athlete's seasonal average value and the local average value of the seven days before. Hence, the calibrated manifestation mirrors divergence from individual baseline instead of pure absolute burden.

On the output stratum, PTO-Net gives out risk probability, preparation degree for the next session, and the suggested training load modification. The first two output results are obtained from two light-weight task headers, while the third one has combined risk, preparation degree and recent change degree together to make a training suggestion. For the avoidance of overabundant formulas, this present paper only keeps the core formulation of the training suggestion, such that it is displayed in Equation (4).

$$\Delta l_{i,t} = a_1 \hat{q}_{i,t+1} - a_2 \hat{p}_{i,t} - a_3 v_{i,t} + b \tag{4}$$

In the equation, $\Delta l_{i,t}$ represents the recommended load adjustment ratio, $\hat{q}_{i,t+1}$ represents the predicted readiness for the next session, $\hat{p}_{i,t}$ represents the risk probability over the next 72 hours, $v_{i,t}$ represents the load fluctuation coefficient over the past 7 days, and a_1, a_2, a_3, and b are learnable parameters. This formula retains the core thought of making training recommendation: when preparation degree goes up, the recommended load has a higher probability to keep stable or have a small rise; When the probability of risk occurrence and short-term fluctuation degree increase, thus the suggested allocation proportion tends to decrease [23-25].

In the concrete carrying out process, the risk task utilizes a two-class classification loss function, but the readiness and load regulating tasks utilize a regression loss. One simple rank restriction is added in the training stage to make sure that the recommended values do not have obvious reverse changes when the recovery state becomes worse or the risk degree rises.

2.3 Intelligent Training Optimization Model

Our experiments have adopted strict temporal splitting for the purpose of preventing future information leakage. All samples are grouped according to athlete ID and arranged in time order, with the first 70% being utilized for training, the next 15% being utilized for validation, and the final 15% being utilized for testing. Sliding windows are produced one by one in each subset, and test data are got rid of from all statistics of the training stage. For the purpose of decreasing

the variance which is related to initialization, every model is operated by using five random seeds, and the mean result is what we report. The unification flow for model comparing, error analyzing, and efficiency assessing is displayed in Figure 3.

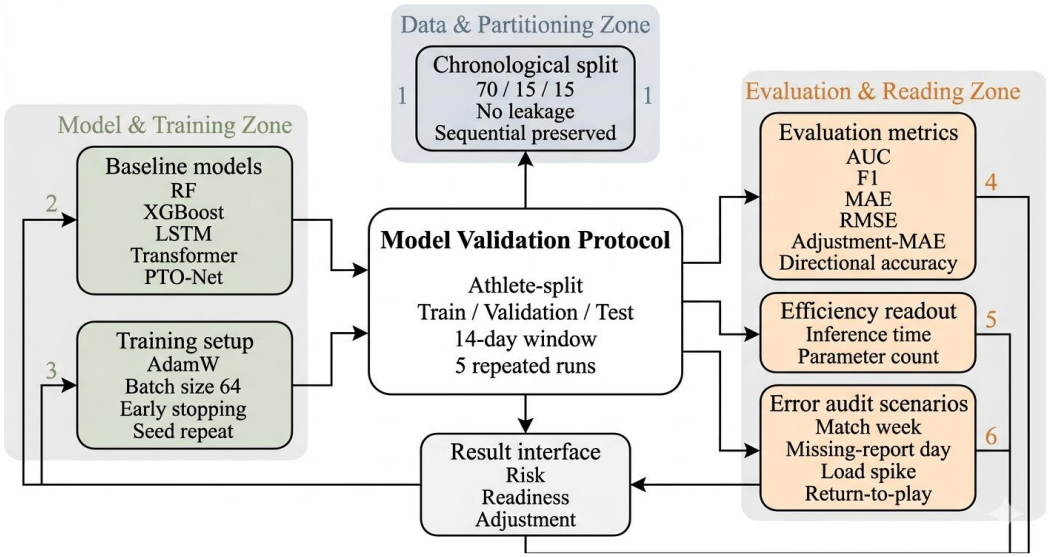

Figure 3: Experimental protocol for comparison, validation, and error audit

For the assessment of PTO-Net, four baseline methods are put forward: Random Forest, XGBoost, LSTM, and Transformer Encoder. All methods employ the identical input items, data division, and window candidate items, with no additional feature engineering work. PTO-Net, LSTM and Transformer are all realized by PyTorch, which uses AdamW optimizer, an initial learning rate of 1×10^{-3}, batch size of 64, and maximum epoch number of 80; The early stopping is to be triggered after 8 validation epochs which have no improvement. The value of Dropout is arranged as 0.2, and the value of weight decay is arranged as 1×10^{-4}. Window lengths which are 7, 14, 21 and 28 days have been undergone testing, hence 14 days is utilized in the main experiment. RF and XGBoost utilize the statistical features which are on window level; RF employs 400 trees, while as for XGBoost, it uses a learning rate of 0.05 and has a maximum depth of 6.

Evaluation metrics were consistent with the task type. For the risk warning task, AUC, Precision, Recall, and F1 were used; for the preparedness prediction task, MAE and RMSE were used; and for the load adjustment task, adjustment-MAE, directional accuracy, and macro-F1 were used. In addition to accuracy, this paper also records the average inference time per sample and the number of parameters to assess deployment costs.To identify the sources of model performance, the subsequent results section will conduct four sets of ablation experiments: removing recovery features, removing individual corrections, removing temporal weighting, and removing adjustment constraints.

The analysis of errors has been organized according to the training context. The test samples are further divided into five kinds of situations: competition weeks, days that have high-load sudden peaks, days where recovery reports are missed, days when people come back after continuous absences, and days that have high fatigue accumulation. This kind of grouping helps us to find out the management conditions in which prediction drift has a bigger possibility to occur.

3 Results and Discussion

3.1 Overall Prediction and Training Recommendation Performance

Risk warnings, preparation forecasts, and burden modifications are not three separate results; Put together, these two aspects hence determine that the degree which training recommendations can be used. Hence, an all-around comparison must take into account both the accuracy of risk identification and the consistency of successive prediction errors and recommendation directions. The comparison of all performance is be showed in Table 2.

Table 2: Overall comparison of prediction and recommendation performance

Model	Risk AUC	Risk F1	Readiness MAE	Readiness RMSE	Adjustment MAE	Directional accuracy	Adjustment Macro-F1
RF	0.781	0.698	6.12	8.01	0.128	0.712	0.684
XGBoost	0.806	0.724	5.74	7.46	0.117	0.741	0.709
LSTM	0.829	0.748	5.21	6.83	0.108	0.768	0.737
Transformer	0.842	0.761	4.97	6.48	0.101	0.781	0.752
PTO-Net	0.871	0.793	4.38	5.63	0.087	0.832	0.804

In Table 2, PTO-Net achieved the best results across all three tasks. Compared with the Transformer baseline that has the nearest performance, the model we put forward increased the risk-alert AUC from 0.842 to 0.871 and Risk F1 from 0.761 to 0.793, hence it shows that the recognition of positive-risk cases has obtained a better balance. In the readiness prediction work, MAE decreased from 4.97 to 4.38, and RMSE decreased from 6.48 to 5.63, this therefore shows that average error and extreme deviation both have been reduced. In the process of load adjustment, the Adjustment MAE has decreased from 0.101 to 0.087, the directional consistency has increased from 78.1% to 83.2%, and thus the Macro-F1 has reached 0.804. These outcomes show that the multi-task design has maintained the effect of each forecasting goal, meanwhile it has made the mapping between state identification and training-load suggestion more compact. To further examine the output boundaries of different models across the three tasks, see Figure 4.

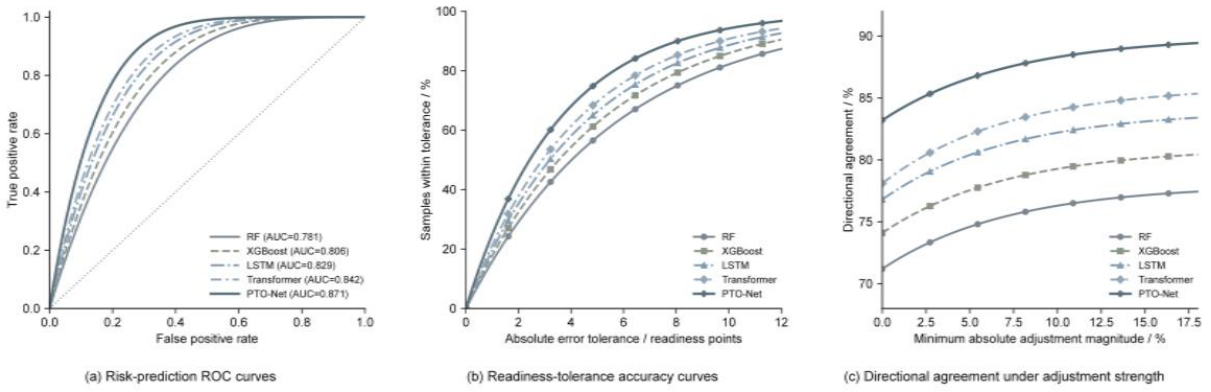

Figure 4: Model performance curves across three prediction tasks

In Figure 4(a), the ROC curve of PTO-Net is always situated on the outer side of the curves of baseline methods through the majority of the threshold range, and retains a higher true positive rate in the region of low false positive, hence it indicates that the capability of early warning discrimination is stronger. In Figure 4(b), the PTO-Net has covered over 70 percent of

the samples that lie inside the ±5-minute readiness tolerance band, when comparing with approximately 65 percent for the Transformer and approximately 60 percent for the LSTM, hence it displays a more concentrated estimation of next-session state. In the Figure 4(c), directional consistency goes up for every model when the smallest adjustment threshold gets bigger, therefore PTO-Net has faster improvement and hence gets to around 88% close to the 10% threshold. This therefore indicates that the model possesses greater stability on samples which demand a clear increase or decrease of load. The mutual effect among load change, restoration condition, and suggested adjustment is displayed in Figure 5.

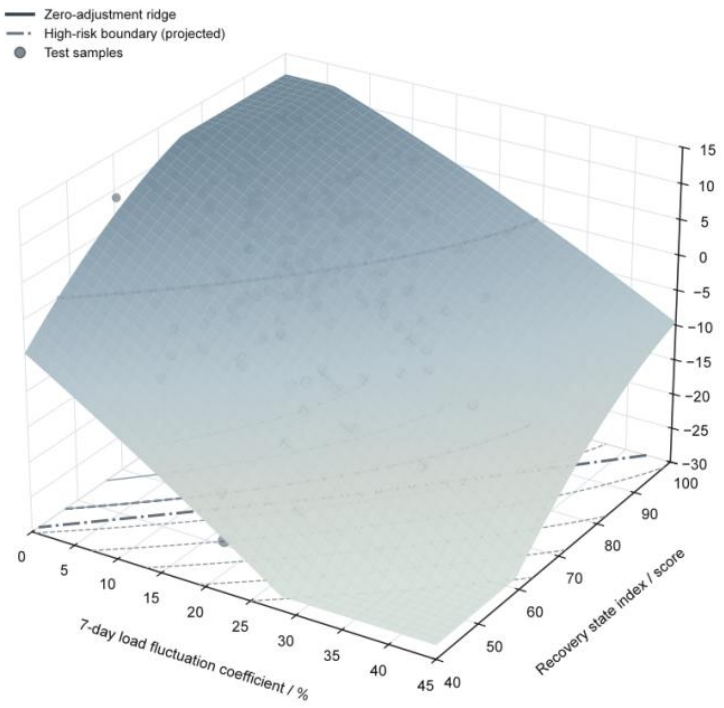

Figure 5: Three-dimensional coupling surface of load fluctuation, recovery state, and recommended training adjustments

The Figure 5 has exhibited a response surface that is clear. When the 7-day load undulation coefficient is under 15% and the recovery index surpasses 80, the suggested adjustment is on the whole near zero or a little positive, it mostly changes from 0% to 8%, this shows keeping the current speed or a gentle increase. When the recovery degree is lower than 60 and the fluctuation magnitude is higher than 25%, hence the surface has an obvious decrease, therefore the suggestions gather between −11% and −26%. When fluctuation gets close to 35%, and recovery approaches 50, the minimum value gets to around −26%, this therefore forms a clear reduction area. The scatter disperse distribution obeys the identical surface shape, with high-danger samples gathered in the low-recovery, high-fluctuation area. This shows that the recommendation is generated by the combined action of undulation and restoration, hence it is not produced by a single fixed threshold.

3.2 Ablation, Temporal Window, and Efficiency Analysis

The whole results indicate that PTO-Net gets the best performance on the main task, but two additional questions still exist: which modules are the cause of this improvement, and whether the improvement comes together with extra calculation load. For answering these questions,

this section carries out examination on module ablation, temporal-window sensitivity, and efficiency limits. The results of ablation and the inference efficiency have been reported by us in Table 3.

Table 3: Ablation results and inference efficiency

Variant	Risk AUC	Readiness MAE	Directional accuracy	Parameters / M	Inference time / ms
Full PTO-Net	0.871	4.38	0.832	2.40	4.9
− Recovery branch	0.819	4.81	0.777	2.33	4.7
− Baseline calibration	0.841	4.57	0.792	2.38	4.8
− Temporal weighting	0.828	4.66	0.787	2.09	4.4
− Adjustment constraint	0.854	4.44	0.806	2.40	4.9

Table 3 has displayed that the biggest performance decline appears after the recovery branch is removed. Risk AUC reduces from 0.871 to 0.819, and direction consistence drops from 83.2% to 77.7%, hence that rehabilitation information directly influences the stability of load recommendation. After the completion of individual baseline correction removal, Risk AUC has a decrease to 0.841, hence this indicates that the processing of athlete-specific tolerance differences under similar loads is weaker. After the elimination of temporal weighting, AUC reduces to 0.828, this shows that time intervals around competition weeks and high-variation days ought not to be handled in an equal way. After we take away the adjustment constraint, the changes of risk and readiness error still keep limited, therefore, the directional consistency falls to 80.6%, hence it shows this constraint mainly gives support to the stability of recommendation. Figure 6 more clearly gives expression to these differences.

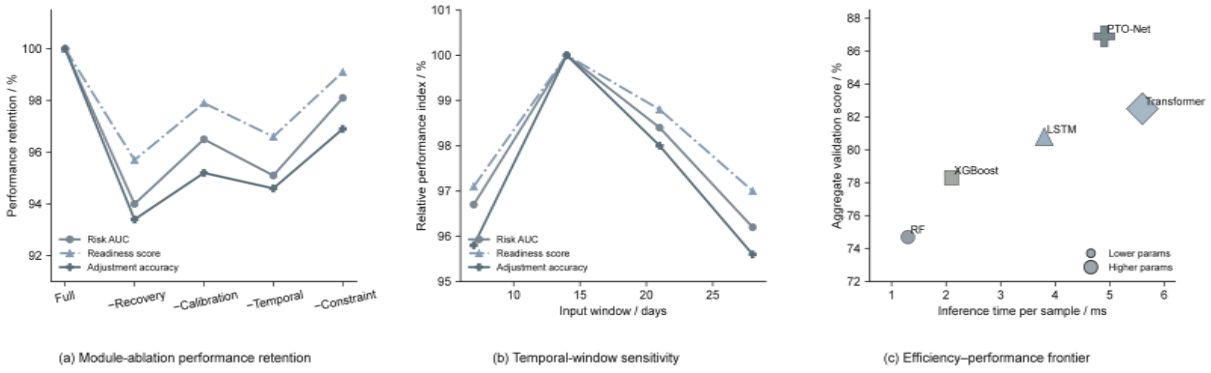

Figure 6: Ablation, Temporal-Window Sensitivity, and Efficiency Frontier

In Figure 6(a), if we remove the recovery branch, this will bring about the biggest simultaneous drop on all the three tasks. The influences of single revision and time weighting are a little smaller, but both still display a continuous downward movement, hence it demonstrates steady contributions to condition expression. In Figure 6(b), the 7-day window gives quicker reaction to short-term change, therefore its whole performance is lower than the performance of the 14-day window. The 21-day and 28-day time periods can include longer cycles, but thus their sensitivity towards the disturbance of recent training becomes decreased. The 14-day time frame still keeps the nearest position to the optimal outcome in all three tasks, hence this shows a more superior equilibrium among weekly competition change, recovery delay, and accumulated training burden. In Figure 6(c), PTO-Net records that the inference time for one single sample is 4.9 ms, which is lower than Transformer's 5.6 ms, therefore it still can

obtain a higher total verification score. This outcome shows that the present design keeps efficiency together with task accomplishment and is enough for group assessment before everyday training courses.

3.3 Error Structure, Case Interpretation, and Deployment Implications

Average measurement indexes can show whether a model has effect, but what truly decides its use possibility is whether it can still give believable outputs in conditions of high training day changeability, in competition weeks, and in situations with not complete data. Hence, we finally have to go beyond average measurement indexes to analyze error structure and explanations on the individual level. Figure 7 give out the error distribution, feature contribution degrees, and case-level adjustment movement paths.

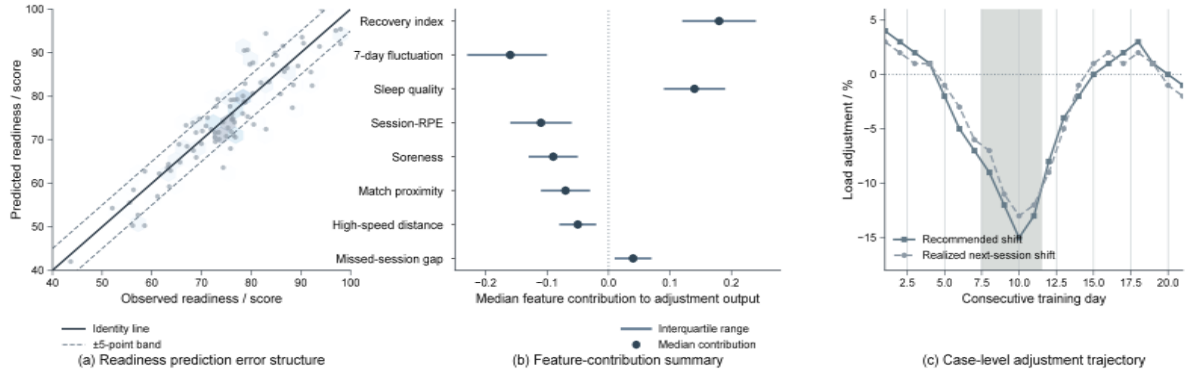

Figure 7: Error structure, feature contribution, and case-level adjustment trajectory

In Figure 7(a), the predictions of readiness gather close to the diagonal line, with most samples locating inside the ±5-point band, which shows that the estimation in middle-range states is stable. Bigger deviations occur mainly in the extreme high and low parts, where the numbers of samples are not enough and situations are often connected with competition weeks or training that aims at recovery. In Figure 7(b), the recovery index has the strongest positive contribution, while the 7-day load fluctuation coefficient gives the most negative contribution, after that comes sleep quality, Session-RPE, and muscle soreness. This ordering accords with training thought: higher recovery and more stable recent load help hold or a little raise training, while bigger short-term change, piled tiredness, and worse pain push the suggestion to go lower. Figure 7(c) carries out the tracing for one athlete's 21-day adjustment path. In the high-risk time window which is from day 8 to day 12, the suggested load has a decrease from -9% to -15%, therefore the actual load of the next session drops from -7% to -13%, hence this shows the model is able to send out early reduction signals when risk is accumulating, and thus it keeps very high consistency with the training decisions made after. Table 4 carries out further decomposition on error sources among different training situations.

Table 4: Scenario-wise error profile and deployment implications

Scenario	Risk F1	Readiness MAE	Adjustment MAE	Deployment Implication
Match week	0.742	4.61	0.094	Recommend joint review with subjective recovery within 48 hours before the match
Missing-report day	0.701	5.22	0.111	Missing report days should be marked with low confidence
Load-spike day	0.768	4.73	0.104	When $\Delta l > 10\%$, recommend manual confirmation
Return-to-play	0.689	5.36	0.119	Re-training phase should be evaluated in conjunction with medical clearance
High fatigue accumulation	0.781	4.42	0.089	Continuous high fatigue over three days can directly trigger observation

In Table 4, the weakest outcomes show themselves in the retraining stage and on days which have missing recovery reports. In the previous situation, Risk F1 is only 0.689, this shows that the model still keeps sensitivity to boundary cases where medical clearance work has been finished but functional condition is still not stable. In the latter case, Readiness MAE increases to 5.22, which indicates that the lack of subjective recovery input will lower the sensitivity to short-term state changes. Through comparison, errors are smaller when fatigue accumulation is high, in which place recovery signals are more continuous and internally consistent.

These findings indicate that PTO-Net is better suited to decision support within training management. On routine training days, it can provide relatively stable risk estimates and load-adjustment suggestions. In retraining periods, under substantial data gaps, or during compressed schedules, its outputs are more appropriate for preliminary screening and priority marking before staff review.

The superiority of PTO-Net originates from the united modeling of load undulation, recovery alteration, and each individual base line. In the whole evaluation, it still stays before the comparison methods, and gives more clear adjustment direction in areas which have features of high risk, low recovery, and big fluctuation. The outcomes also indicate that training optimization is strongly constrained by the context. In the process of retraining, competition weeks and time periods where monitoring is not complete, the stability of output is formed together by management restrictions and the completeness of data. Therefore its actual value lies in firm support inside fixed use limits, especially for daily time arrangement, before-meeting check, and recovery follow-up.

4 Conclusion

This study develops an intelligent framework for daily training decisions in athlete management and evaluates it with public monitoring data. The results show that load, recovery, and individual difference can be integrated within one decision process, so that risk warning, state evaluation, and load adjustment are generated in a form that is easier to use in practice.

(1) A unified athlete-day data structure has integrated training logs, recovery self-reports, attendance records, and contextual environment variables into continuous sample sequences. A sliding-window plan has kept short-term wave motion and recent buildup, hence it offers a common input foundation for risk reminding, preparation forecast, and burden regulation.

(2) PTO-Net has obtained the best whole performance. The risk early warning method

obtained an AUC value of 0.871, and its Risk F1 value was 0.793; The readiness prediction work has obtained a MAE value of 4.38, and a RMSE value of 5.63; The load adjusting work obtained a MAE value of 0.087 and 83.2% direction consistency, therefore it has better performance than RF, XGBoost, LSTM, and Transformer. The three-dimensional curved surface response hence displayed more distinct load-decrease signals under the condition of lower degree of recovery and bigger short-term fluctuation. Ablation experiment outcomes have found that the recovery branch, individual baseline rectification, and time weight are the main origins of performance, thus confirming the combined value of fluctuation, recovery reaction, and tolerance which is specific to athletes.

(3) The obtained outcomes also delimit the present application scope boundary. Errors have an increase when retraining time periods, competition weeks, and situations that have much missing recovery data exist, this shows the model still depends on data completeness and management background. The subsequent work should bring in more fine-divided physiological observation, season-level transfer study study, and multi-group outside verification to promote robustness in sport environments, competition density, and training arrangement.

About the Author

Yangyang Li (1991.2-) is male, Han ethnic group, was born in Wuhan, has Master degree, is lecturer, got Master degree from Wuhan Institute of Physical Education, works as lecturer at Wuhan Technical College of Communications, his research direction is Pedagogy.

You Yang, who was born in March 1992, is a female of Han ethnic group, who was given birth in Wuhan, holds a Master degree, is a teaching lecturer, who obtained Master degree from Wuhan Institute of Physical Education, works as lecturer at Wuhan Qingchuan University, whose research direction is physical education training and teaching.

References

[1] International Olympic Committee. (2024). Olympic AI agenda. International Olympic Committee.

[2] Zhou, D., Keogh, J. W. L., Ma, Y., et al. (2025). Artificial intelligence in sport: A narrative review of applications, challenges and future trends. Journal of Sports Sciences, 1-16.

[3] Reis, F. J. J., Alaiti, R. K., Vallio, C. S., et al. (2024). Artificial intelligence and machine learning approaches in sports: Concepts, applications, challenges, and future perspectives. Brazilian Journal of Physical Therapy, 28(3), 101083.

[4] Bourdon, P. C., Cardinale, M., Murray, A., et al. (2017). Monitoring athlete training loads: Consensus statement. International Journal of Sports Physiology and Performance, 12(Suppl 2), S2-161-S2-170.

[5] Impellizzeri, F. M., Marcora, S. M., & Coutts, A. J. (2019). Internal and external training load: 15 years on. International Journal of Sports Physiology and Performance, 14(2), 270-273.

[6] Chidambaram, S., Maheswaran, Y., Patel, K., et al. (2022). Using artificial intelligence-enhanced sensing and wearable technology in sports medicine and performance

optimisation. Sensors, 22(18), 6920.

[7] Kim, J.-H., Kim, J., Kang, H., et al. (2025). Ethical implications of artificial intelligence in sport: A systematic scoping review. Journal of Sport and Health Science, 14, 101047.

[8] Midoglu, C., Winther, A. K., Boeker, M., et al. (2024). A large-scale multivariate soccer athlete health, performance, and position monitoring dataset. Scientific Data, 11, 553.

[9] Halson, S. L. (2014). Monitoring training load to understand fatigue in athletes. Sports Medicine, 44(Suppl 2), S139-S147.

[10] Seçkin, A. Ç., Ateş, B., & Seçkin, M. (2023). Review on wearable technology in sports: Concepts, challenges and opportunities. Applied Sciences, 13(18), 10399.

[11] White, M., De Lazzari, B., Bezodis, N., et al. (2024). Wearable sensors for athletic performance: A comparison of discrete and continuous feature-extraction methods for prediction models. Mathematics, 12(12), 1853.

[12] Wang, C., Tang, M., Xiao, K., et al. (2024). Optimization system for training efficiency and load balance based on the fusion of heart rate and inertial sensors. Preventive Medicine Reports, 41, 102710.

[13] Jaspers, A., De Beéck, T. O., Brink, M. S., et al. (2018). Relationships between the external and internal training load in professional soccer: What can we learn from machine learning? International Journal of Sports Physiology and Performance, 13(5), 625-630.

[14] Chen, T., & Guestrin, C. (2016). XGBoost: A scalable tree boosting system. In Proceedings of the 22nd ACM SIGKDD International Conference on Knowledge Discovery and Data Mining (pp. 785-794).

[15] Hochreiter, S., & Schmidhuber, J. (1997). Long short-term memory. Neural Computation, 9(8), 1735-1780.

[16] Vaswani, A., Shazeer, N., Parmar, N., et al. (2017). Attention is all you need. In Advances in Neural Information Processing Systems (Vol. 30, pp. 5998-6008).

[17] Lundberg, S. M., & Lee, S.-I. (2017). A unified approach to interpreting model predictions. In Advances in Neural Information Processing Systems (Vol. 30, pp. 4765-4774).

[18] Barredo Arrieta, A., Díaz-Rodríguez, N., Del Ser, J., et al. (2020). Explainable artificial intelligence (XAI): Concepts, taxonomies, opportunities and challenges toward responsible AI. Information Fusion, 58, 82-115.

[19] Tsilimigkras, T., Kakkos, I., Matsopoulos, G. K., et al. (2024). Enhancing sports injury risk assessment in soccer through machine learning and training load analysis. Journal of Sports Science and Medicine, 23, 537-547.

[20] Leckey, C., Van Dyk, N., Doherty, C., et al. (2025). Machine learning approaches to injury risk prediction in sport: A scoping review with evidence synthesis. British Journal of

Sports Medicine, 59(7), 491-500.

[21] Ye, X., Huang, Y., Bai, Z., et al. (2023). A novel approach for sports injury risk prediction: Based on time-series image encoding and deep learning. Frontiers in Physiology, 14, 1174525.

[22] Fang, D., & Chen, C. (2025). Sports injury risk prediction based on temporal graph encoding and graph neural networks: A cross-sport transfer learning framework. Scientific Reports, 15, 37656.

[23] Van Eetvelde, H., Mendonça, L. D., Ley, C., et al. (2021). Machine learning methods in sport injury prediction and prevention: A systematic review. Journal of Experimental Orthopaedics, 8, 27.

[24] Nassis, G. P., Verhagen, E., Brito, J., et al. (2023). A review of machine learning applications in soccer with an emphasis on injury risk. Biology of Sport, 40(1), 233-239.

[25] Rossi, A., Pappalardo, L., Cintia, P., et al. (2018). Effective injury forecasting in soccer with GPS training data and machine learning. PLOS ONE, 13(7), e0201264.